

# Giant oscillations of energy levels in mesoscopic superconductors

N. B. Kopnin<sup>(1;2)</sup>, A. S. Melnikov<sup>(3;4)</sup>, V. I. Pozdnyakova<sup>(3)</sup>,  
D. A. Ryzhov<sup>(3)</sup>, I. A. Shereshevskii<sup>(3)</sup>, and V. M. Vinokur<sup>(4)</sup>

<sup>(1)</sup> Low Temperature Laboratory, Helsinki University of Technology, P.O. Box 2200, FIN-02015 HUT, Finland,

<sup>(2)</sup> L. D. Landau Institute for Theoretical Physics, 117940 Moscow, Russia

<sup>(3)</sup> Institute for Physics of Microstructures, Russian Academy of Sciences, 603950, Nizhny Novgorod, GSP-105, Russia,

<sup>(4)</sup> Argonne National Laboratory, Argonne, Illinois 60439

(Dated: March 23, 2024)

The interplay of geometrical and Andreev quantization in mesoscopic superconductors leads to giant mesoscopic oscillations of energy levels as functions of the Fermi momentum and/or sample size. Quantization rules are formulated for closed quasiparticle trajectories in the presence of normal scattering at the sample boundaries. Two generic examples of mesoscopic systems are studied: (i) one dimensional Andreev states in a quantum box, (ii) a single vortex in a mesoscopic cylinder.

PACS numbers: 74.78.-w, 74.25.Fy, 74.25.Dp, 74.50.+r

A normal cavity in a superconductor sample confines normal carriers due to their Andreev reflection from the walls formed by the superconductor order parameter. In the present Letter we show that Andreev levels in samples with sizes comparable to the coherence length exhibit giant mesoscopic oscillations as functions of the Fermi momentum  $k_F$  and/or sample dimensions with an amplitude that substantially exceeds the interlevel spacing they would have in bulk samples. For illustration, let us compare the effects of geometrical confinement for bound states in normal and superconducting systems. Consider one dimensional motion of a particle in a potential well of finite depth. The particle wave function oscillates as  $e^{ikx}$  in classically accessible and decays exponentially in forbidden regions respectively. Placing the entire system into a quantum box of the size  $L_0$  larger than the width of the well,  $d$ , makes the wave function to vanish at the box boundaries. This is equivalent to a decrease in the effective width of the well and results in a slight modification of the bound states. Let us now take a sandwich-like structure of a total thickness  $L_0$  where the normal (N) slab of a thickness  $d$  is confined between two superconducting (S) layers with a certain order parameter phase difference between them (see Fig. 1), and consider the effect of the geometrical confinement on Andreev states with energies below the superconducting gap  $\Delta$ . As before, the particle/hole wave functions in the N region oscillate with  $k = k_F = \sqrt{2mE}$ , where  $v_F$  is the Fermi velocity. However, in contrast to the previous example, the wave functions oscillate further into the S layers with the period of  $2/k_F$  and with the amplitude slowly decaying on the scale of the superconductor coherence length  $\xi_0 = \hbar v_F / \Delta$ . Only when the particle in the box is exactly in the geometrical resonance,  $k_F L_0 = \pi n$ , i.e., when one of its normal-state energy levels coincides with the Fermi level, the Andreev states do not feel the external boundaries, see Fig. 1. When the particle is out of resonance,  $\sin(k_F L_0) \neq 0$ , to satisfy the zero boundary conditions an adjustment of either the wave vector in the N region

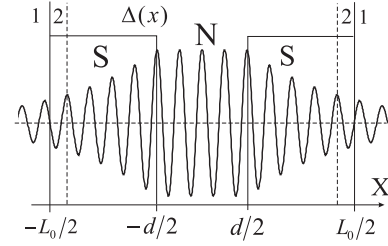


FIG. 1: Andreev states in an SNS structure placed in a quantum box of length  $L_0$ . Solid (1) and dashed (2) lines show the positions of the box boundaries for resonance and off-resonance situations, respectively.

by  $k = \sqrt{2mE} = \sqrt{2m(E - \Delta)}$  (for  $d > \xi_0$ ) or of the phase shift between the electrons and holes by  $\arccos(\Delta/E)$  (for  $d < \xi_0$ ) is needed. Thus, the deviations in energy are large and may compare to  $\Delta$  for  $d < \xi_0$ .

We thus see that the interplay between geometrical and Andreev quantization results in giant oscillations of the Andreev levels as functions of  $k_F L_0$  with an amplitude of the order of  $\Delta$ . The amplitude decreases exponentially as a function of the distance from the external boundary to the Andreev turning point of a particle at the NS interface. This oscillatory phenomenon can be viewed as a generalization of geometrical effects caused by the presence of impurity atoms in vortex cores [1] and Tomash oscillations in  $\text{InSb}$  and finite-size type-II superconductors [2, 3] but with the enormously amplified magnitude. The mesoscopic oscillations strongly affect both thermodynamic and transport properties of nanoscale superconductors that are the focus of current experimental and theoretical research (see [3, 4, 5] and references therein). Interference effects of similar origin have been previously studied for hybrid NS systems with multiple semi-transparent insulator potential barriers [6] (see also [4] for a review).

Closed trajectories. { The one dimensional physics in a quantum box is related to the concept of closed tra-

jectories whose impact on the validity of the quasichasical description of superconductivity is discussed in [7]. Making use of this concept enables one to generalize the above picture to higher dimensions. A standard semiclassical approach to superconductors is formulated for the quasiparticle motion along the beam  $\mathbf{r} = \mathbf{S}$  where  $\mathbf{S}$  is the normal-state eikonal,  $\nabla \mathbf{S} = \mathbf{k}_F$ . The wave function of fermionic excitations has two components in the particle-hole space  $\hat{\psi} = (u; v)$  and can be written as  $\hat{\psi} = \hat{\psi} e^{iS}$ , where  $\hat{\psi}$  is the envelope function varying slowly over the Fermi wavelength. Generally, the phase  $S$  gained along open trajectories does not affect excitation characteristics such as energy levels or density of states (DOS). However, the closed trajectories formed due to boundaries, impurity potentials, and/or in an applied magnetic field, do influence the energy spectrum.

Consider a closed trajectory of the length  $L$ . The wave function  $\hat{\psi}$  should be single valued, which gives

$$\hat{\psi}(s) = \hat{\psi}(s + L) e^{iS(L)}; \quad (1)$$

where  $S(L) = \int_0^L \mathbf{k}_F \cdot d\mathbf{r} = k_F L$  is independent of the arc length  $s$  along the trajectory. Equation (1) suggests that the initial problem is equivalent to the problem of an unbounded motion of a particle in the periodic gap potential  $\psi(s) = \psi(s + L)$  for the proper choice of the quasimomentum  $q$  (see below). In the latter case the wave function satisfies the Bloch theorem

$$\hat{\psi}_q(s + L) = e^{iqL} \hat{\psi}_q(s); \quad (2)$$

while the energy is a periodic function of  $q$ :  $\epsilon(q + 2\pi/L) = \epsilon(q)$ . Comparing Eqs. (1) and (2) we find  $q = [2M - S(L)]/L$ , where  $M$  is a large integer chosen such that  $q$  belongs to the first Brillouin zone. Consider two examples: (i) States with  $\epsilon > \epsilon_c = \text{const}$  will have the spectrum  $\epsilon^2 = \epsilon_c^2 + \sim v_F^2 (2M - L k_F)^2$  where  $M^0 = M - N$ ,  $N$  being the number of the energy band. This spectrum results in Tomash oscillations [2, 3]. (ii) For sub-gap states the correspondence between the spectrum in a mesoscopic superconductor and in a bulk sample can be easily established for  $L \gg L_0$ . Let  $\psi^{(0)}$  be an Andreev bound state for  $L \rightarrow \infty$ . The tight binding approximation in the equivalent periodic problem yields

$$\psi = \psi^{(0)} + (\cos q + C); \quad (3)$$

where the band width  $\epsilon_L$  is proportional to the exponential overlap of the decaying functions for the sub-gap states,  $\psi^{(0)} \sim e^{-L/L_0}$ , and  $C = qL + \dots$ . The parameters  $\epsilon_c$  and  $C$  depend on the particular problem. Since  $\cos q = \cos(k_F L)$ , the energy level oscillates rapidly as a function of  $k_F L$ . The amplitude of oscillations can well exceed the value of  $\psi^{(0)}$  itself, provided the loop length  $L$  is not much larger than  $L_0$ .

The relative contribution of such oscillations to bulk properties depends on the relative weight of closed trajectories allowed by the particular sample geometry. Below we focus on two problems where these contributions

are critical: (i) one dimensional (1D) Andreev states in a quantum box (this problem has been discussed briefly in the introduction), and (ii) energy states in a vortex core placed in a clean mesoscopic cylinder of a finite radius. In both cases the dimensions of the system are assumed comparable to  $L_0$ .

1D Andreev bound states in a quantum box. Consider a quantum point contact which is transparent to a few modes  $N_c$  passing from one superconducting lead to another. We further assume that these modes are localized within the device by specular reflections at the boundaries of the leads which are separated by a distance  $L_0$ . The leads contain also large numbers of other modes  $N_{\text{lead}} \gg N_c$ , which take part in the superconducting pairing. The leads can be connected, via some of the modes  $N_{\text{lead}}$ , to an external superconducting circuit to control the phase difference between them. A possible realization of this device is an adiabatic constriction of the type discussed in [8]. For the modes  $N_c$  that pass through the constriction but are confined within the box of the size  $L_0$ , the quantum mechanical problem corresponds exactly to that in Fig. 1 for the limit  $d \rightarrow 0$ .

We assume a step-like gap potential  $\Delta(x) = \Delta_0 e^{i \text{sign}(x)}$ . The confinement couples the states with opposite momenta and creates a closed trajectory loop of the length  $L = 2L_0$ . In the  $S$  region one has the waves  $e^{iqx}$  and  $e^{-iqx}$ , where  $q = k_x - i\gamma$ ,  $\gamma = \frac{\Delta_0^2}{2\epsilon_0^2} \sim v_x^2$ ,  $k_x$  and  $v_x$  are the particle momentum and velocity projections on the  $x$  axis. We choose here  $\gamma \ll \gamma_0$ , however, the same expressions hold also for  $\gamma \gg \gamma_0$  with an imaginary  $\gamma$ . Matching these wave functions yields the dispersion relation

$$\epsilon^2 = \epsilon_0^2 (1 - T \sin^2(\gamma/2)) : \quad (4)$$

The transmission coefficient  $T = (1 + A)^{-1}$ , and  $A = \sin^2(k_x L_0) = \sinh^2(\gamma L_0)$ . For  $L_0 \gg L_0^0$  and  $\gamma \ll \gamma_0$ , Eq. (4) looks like Eq. (3) in accordance with the general arguments above. Equation (4) has a familiar form [4] of the spectrum for a contact with the double barrier of strength  $A$ . It describes mesoscopic fluctuations and accounts for the resonance transmission at  $\sin(k_x L_0) = 0$ . However, the effect of spectrum modifications is not restricted to mere renormalization of the barrier strength. Qualitatively new features appear due to the energy dependence of the transmission coefficient  $T$ . Because of the geometrical quantization, the spectrum for  $\gamma \gg \gamma_0$  is no longer a continuum and cannot be separated from the phase-dependent sub-gap state; instead, we obtain a set of  $\gamma$ -dependent discrete levels in the entire energy range. For a short box  $L_0 \sim L_0^0$ , the lowest energy level is

$$\epsilon_0^2(\gamma) = \epsilon_0^2 [\cos^2(\gamma/2) + (\gamma v_x = \gamma_0 L_0)^2 \sin^2(k_x L_0)] :$$

For  $\gamma \gg \gamma_0$ , the levels transform into the  $\gamma$ -independent spectrum in a normal metal box:  $(-k_x - n\pi/L_0) = -n\pi/L_0$ , where  $n$  is an integer. Each  $\gamma$ -dependent level provides

an oscillatory contribution to the supercurrent [9]:

$$I_n(\tau) = \frac{2ed_n(\tau)}{\sim d} \tanh \frac{n(\tau)}{2T}; \quad (5)$$

where only  $n > 0$  are taken. Note that the supercurrent in Eq. (5) is transported by the modes which, in the normal state, are localized and do not carry current. In the superconducting state, however, the current along the localized modes  $N_c$  appears due to the conversion over distances  $\sim \lambda_{L0}$  of the supercurrent from delocalized modes  $N_{lead}$ . The analysis of Eq. (4) shows that the strongest dependence is realized for the lowest energy state which thus dominates the current.

Vortex core states in a mesoscopic superconductor. We consider now low energy core states in a single vortex introduced into the center of a mesoscopic cylinder of a radius  $R \ll \lambda_0$  with the quasiparticle mean free path  $\lambda \ll R$ . Bogoliubov-de Gennes (BdG) equations read

$$\frac{\hbar^2}{2m} \nabla^2 \psi + E_F + \hat{\sigma} \psi = \hat{\sigma}_z \psi;$$

where  $\hat{\sigma} = j(r) \hat{\sigma}_y$ ,  $\hat{\sigma}_i$  are Pauli matrices, and  $r, \phi, z$  are cylindrical coordinates with the  $z$  axis parallel to the cylinder axis. The gap  $j(r)$  saturates at  $\Delta_0$  far from the vortex axis. The vector potential here is negligible for an extreme type-II superconductor. We look for a solution  $\psi = e^{i\phi} \hat{U}$  with a given half-integer angular momentum  $\phi$ . If the superconducting cylinder is surrounded by an insulator, the boundary condition requires  $\hat{U}(R; z) = 0$ .

We find the energy spectrum both analytically and numerically. For numerical computations we use a matrix representation of the BdG operator in the basis of the eigenstates with a given momentum  $k_z$  along the  $z$  axis for a normal metal cylinder of the radius  $R$ . We truncate the infinite matrix keeping the number of eigenstates larger than the number of propagating modes in the normal metal waveguide. The obtained  $k_z$ -dependent matrix is diagonalized yielding the energy spectrum for a vortex. We approximate the gap by  $j(r) = \Delta_0 r^2 / (r^2 + \frac{\lambda^2}{4})$ , choosing  $\lambda = \lambda_0$  without the loss of generality. The calculated spectra do not depend qualitatively on the exact shape of  $j(r)$ . Shown in Fig. 2 are typical energy spectra calculated for a realistic material parameter  $\Delta_0/E_F = 0.01$ .

The analytical description is based on a standard quasiclassical scheme [10] modified to take account of the proper phases [11] of radial waves for small values of  $\phi$ :

$$\hat{U} = e^{ik_z z} H_{\phi + \frac{1}{2}}^{(1)}(k_r r) \hat{w}^{(+)} + e^{ik_z z} H_{\phi + \frac{1}{2}}^{(2)}(k_r r) \hat{w}^{(-)};$$

where  $H_1^{(1,2)}$  are the Hankel functions,  $k_r^2 + k_z^2 = k_F^2$ , and  $\hat{w} = (w_1; w_2)$  are slow functions of  $r$ . Solving equations for the envelopes  $\hat{w}^{(\pm)}$  one can construct functions

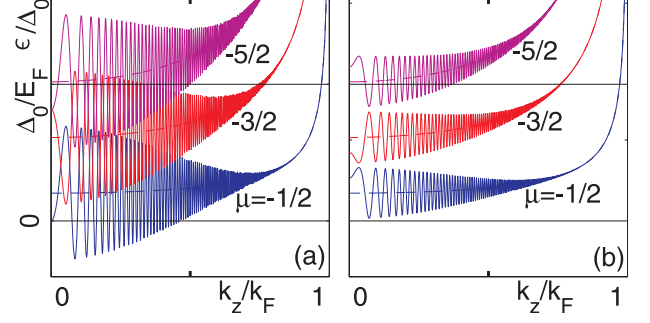


FIG. 2: The energy spectra (solid lines) for a vortex in a mesoscopic cylinder with (a)  $R = 3.5$  and (b)  $R = 4.0$  as functions of  $k_z$ . The CdGM energy spectra are shown by the corresponding dashed lines.

$\hat{w}^>$  and  $\hat{w}^<$  decaying at different ends of the trajectory passing by the vortex [12]. The wave function in a cylinder is the superposition  $\hat{w} = A_> \hat{w}^> + A_< \hat{w}^<$ . The boundary condition at  $r = R$  couples the incoming and outgoing waves which leads to formation of a closed trajectory loop for one-dimensional motion along  $r$ . The solvability condition of the two linear homogeneous equations for two constants  $A_>$  and  $A_<$  gives the bound state energy  $\epsilon(k_r)$  in the form of Eq. (3) where  $\epsilon = \Delta_0 / \cosh[2K(R)]$ ,  $K = 2k_r R + \pi/2$ ,  $C = 0$ , and  $\epsilon^{(0)} = \epsilon(k_r)$  is the Caroli-de Gennes-Matricon (CdGM) energy [10] for a vortex in a bulk superconductor,

$$\epsilon(k_r) = \frac{2m\Delta_0}{\hbar^2 k_r^2} \int_0^R j(r) j(r) e^{2K(r)} dr;$$

$$K(r) = \frac{m}{\hbar^2 k_r} \int_0^r j(r') j(r') dr'; \quad \epsilon = \frac{2m\Delta_0}{\hbar^2 k_r} \int_0^R e^{2K(r)} dr;$$

These analytical expressions are in a very good agreement with our numerical results. The last term in Eq. (3) describes the mesoscopic level fluctuations. Their amplitude  $\epsilon(k_r)$  is much larger than the CdGM level spacing  $\epsilon^{(0)} = \Delta_0/E_F$  if  $R$  is not exceedingly larger than  $\lambda_0$ . Different levels can cross each other because they belong to different angular momenta. The fluctuating levels also can cross zero for not very high  $\phi$ . The amplitude  $\epsilon(k_r)$  decreases as  $k_z$  approaches  $k_F$  since  $\cosh[2K(R)]$  in it grows exponentially as  $k_r$  decreases. Note that in a layered two-dimensional superconductor the amplitude  $\epsilon(k_r)$  is constant corresponding to  $k_z = 0$ . For later use, we define the critical radius  $R_c$  for which the maximum amplitude of oscillations  $\epsilon(k_F)$  is equal to half of the maximum distance between the CdGM states  $\epsilon^{(0)} = \Delta_0/E_F$ . According to Fig. 2(b) the radius  $R = 4\lambda_0$  is slightly larger than  $R_c$  for  $\Delta_0/E_F = 0.01$ .

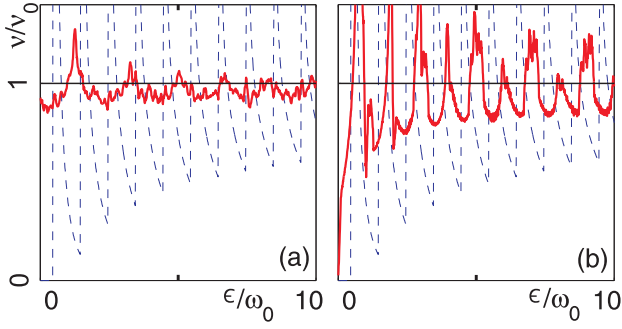


FIG. 3: Solid lines: The DOS for (a)  $R = R_0 = 2.5$  and (b)  $R = R_0 = 4$ . The CdGM DOS is shown by dashed line.

Density of vortex core states. Consider a sample radius  $R < R_c$  such that  $(k_F) > \epsilon_0$ . According to Fig. 2 (a), we divide the range  $0 < k_r < k_F$  into the region of large oscillations  $k_r < k_r < k_F$ , where  $(k_r) \gg \epsilon_0(k_r)$ , and the region  $0 < k_r < k_r$ , where levels are smooth functions of  $k_r$  close to the CdGM form  $\epsilon_0^{(0)}(k_r)$ . The total DOS is a sum  $\nu = \nu_1 + \nu_2$  of contributions from the both regions. In the region  $k_r < k_r < k_F$ , a large number of levels with different  $k_r$  cross the constant energy line many times so that the continuous approximation is appropriate. Therefore,  $\nu_1$  is equal to the CdGM DOS averaged over a large number of angular momentum eigenstates:

$$\nu_1(k_r) = \frac{1}{2\pi} \int_{k_r}^{k_F} \frac{k_r dk_r}{\epsilon_0(k_r) k_F^2 - k_r^2} \quad (6)$$

(per spin projection). It provides a background zero-energy DOS due to mesoscopic level fluctuations. The term  $\nu_2(k_r)$  is a sum of peaks positioned at  $\epsilon_0^{(0)}(k_r)$  with the energy period  $\epsilon_0(k_r)$  larger than the CdGM minigap  $\epsilon_0$ . In the limit  $\epsilon_0(k_r) \gg \epsilon_0$  the term  $\nu_2(k_r)$  saturates at the value determined by the same integral as in Eq. (6) but taken within the limits 0 to  $k_r$ . Therefore, the total DOS saturates at the averaged CdGM DOS  $\nu_0 = \nu_1(0)$ .

If  $R > R_c$  but the amplitude of oscillations is still comparable to  $\epsilon_0$ , there are many roots of  $\epsilon_0(k_r) = \epsilon_0$  for a given  $\epsilon_0$ , such that the effective minigap is  $\epsilon_{min} = \epsilon_0/2$  ( $k_F$ ). It vanishes for  $R = R_c$ .

To simplify our equations we approximate the CdGM interlevel spacing as  $\epsilon_0(k_r) = (k_F - k_r)\epsilon_0$  while  $K(R) = (R/R_0)(k_F - k_r)$  with  $R_0 = 1$ . We end  $k_F = R/R_c$  and  $R_c = (\epsilon_0/2) \ln(\epsilon_0/\epsilon_0)$ . The period of DOS oscillations is thus  $\epsilon_0(k_r) = \epsilon_0 R_c/R$ . The background DOS is

$$\nu_1 = \nu_0 \left( 1 - \frac{h}{2\pi} \arcsin \frac{p}{1 - \frac{h}{2\pi}} \right);$$

where  $\nu_0 = k_F/4\epsilon_0$  and  $\epsilon_0 = R/R_c$ . It vanishes for  $\epsilon_0 = 1$ .

We calculated the DOS numerically using the obtained analytical expressions for the energy spectrum. To exclude a large number of van Hove singularities the DOS

was averaged over a small energy interval  $\epsilon_0 = 0.1\epsilon_0$ . The results for  $R < R_c$  and  $R = R_c$  shown in Fig. 3 (a) and (b), respectively, are in good agreement with the above analytical estimates. In particular, the period of oscillations in Fig. 3 (a) is approximately 1.5 times larger than the period  $\epsilon_0$  for the CdGM DOS in the bulk, which agrees with the value of the cylinder radius  $R = R_c = 1.5$ . At the same time, the period in Fig. 3 (b) almost coincides with  $\epsilon_0$ ; in addition, the minigap here vanishes. These features well correspond to  $R$  being close to  $R_c$ .

To summarize, we predict a profound effect of geometrical quantization on Andreev states in mesoscopic superconductors, which exhibit giant oscillations as functions of the particle momentum and the sample size. In particular, the geometrical quantization results in appearance of zero energy modes for vortex core states. We discussed the case of ideal sample surfaces, however one expects all the essential conclusions to hold for atomically smooth sample surfaces as well. The spectrum oscillations can be observed by scanning tunnelling spectroscopy with high energy resolution and by transport measurements in weak links.

We thank A. Andronov, S. Sharov, and A. Shelankov for valuable discussions. This work was supported, in part, by the US DOE Office of Science, contract No. W-31-109-ENG-38, by Russian Foundation for Basic Research, by Program "Quantum Macrophysics" of Russian Academy of Sciences, by Russian Presidential Program under grant No. MD-141.2003.02, by Russian Science Support Foundation, by the "Dynasty" Foundation, and by the Russian Ministry of Science and Education.

- 
- [1] A. I. Larkin and Yu. N. Ovchinnikov, Phys. Rev. B 57, 5457 (1998); A. A. Koulakov and A. I. Larkin, Phys. Rev. B 59, 12021 (1999).
  - [2] W. J. Tomasz, Phys. Rev. Lett. 15, 672 (1965); W. L. McDillan and P. W. Anderson, Phys. Rev. Lett. 16, 85 (1966).
  - [3] K. Tanaka, I. Robel, and B. Janko, PNAS, 99, 5233 (2002).
  - [4] A. A. Golubov, M. Yu. Kupriyanov and E. Il'ichev, Rev. Mod. Phys. 76, 411 (2004).
  - [5] A. S. Mel'nikov and V. M. Vinokur, Nature, 415, 60 (2002); Phys. Rev. B 65, 224514 (2002).
  - [6] A. V. Galaktionov and A. D. Zaikin, Phys. Rev. B 65, 184507 (2002).
  - [7] M. Ozana and A. Shelankov, Phys. Rev. B 65, 014510 (2001).
  - [8] C. W. J. Beenakker and H. van Houten, Phys. Rev. Lett. 66, 3056 (1991).
  - [9] C. W. J. Beenakker, Phys. Rev. Lett. 67, 3836 (1991).
  - [10] C. Caroli, P. G. de Gennes, J. Matricon, Phys. Lett. 9, 307 (1964).
  - [11] M. Skvortsov, unpublished.
  - [12] N. B. Kopnin, A. S. Mel'nikov, and V. M. Vinokur, Phys. Rev. B 68, 054528 (2003).